JOURNAL OF SOLID STATE CHEMISTRY 117, 48–54 (1995)

Synthesis, Structure and Magnetic Susceptibility of the Oxynitride Spinel $Mn_2(MnTa_3)N_{6-\delta}O_{2+\delta}$, $0 \leq \delta \leq 1$

J. Grins,[1] P.-O. Käll, and G. Svensson

Department of Inorganic Chemistry, Arrhenius Laboratory, Stockholm University, S-106 91 Stockholm, Sweden

Received November 7, 1994; accepted December 5, 1994

The oxynitride spinel $Mn_2(MnTa_3)N_{6-\delta}O_{2+\delta}$, with $0 \leq \delta \leq 1$, has been synthesized at 1175 K by ammonolysis of a mixture of a Ta-containing xerogel and $Mn(OAc)_2 \cdot 4H_2O$. The N content was determined by combustion analysis and thermogravimetric oxidation, yielding a composition confined between $Mn_2(MnTa_3)N_6O_2$ ($\delta = 0$) and $Mn_2(MnTa_3)N_5O_3$ ($\delta = 1$). The structure is cubic, with space group $Fd3m$ and $a = 8.8353(3)$ Å. It was refined using the Rietveld technique and neutron powder diffraction data collected at room temperature and 15 K, to $R_F = 2.9$ and 3.8%, respectively. The tetrahedral sites are occupied only by Mn atoms and the octahedral sites statistically by 25% Mn and 75% Ta atoms. The N and O atoms are randomly distributed over the anion sites. The magnetic susceptibility exhibits a maximum at 29 K and a Curie–Weiss behavior at higher temperatures with $\theta_a = -250(20)$ K and $\mu_{eff} = 5.7(2)$ Bohr magnetons per Mn atom. The neutron powder diffraction data collected at 15 K showed no evidence of magnetic ordering. A NaCl-type phase with $a = 4.4382(2)$ Å and tentative composition $Mn_{0.8}Ta_{0.2}(O,N)$ was observed in preparations at 1175 K. A hexagonal $Mn_4Ta_2(O,N)_x$ phase with cell dimensions $a = 5.3024(4)$ Å, $c = 14.493(2)$ Å was obtained at 973 K.

INTRODUCTION

There has been an increasing interest in synthesis and characterization of nitrides and oxynitrides during recent years. Different synthetic routes have been utilized, one of them being ammonolysis of suitable precursors. Several new Ta–Zr oxynitride phases were recently synthesized by us at relatively low temperatures, ≤ 1273 K, by ammonolysis of xerogels containing both Ta and Zr (1).

During a subsequent investigation of phase formation in the extended system Mn–Ta–Zr–(O,N), a new oxynitride spinel was encountered. The majority of known spinels AB_2X_4 (2, 3) are oxides, but the category also includes compounds where the X atoms are S, Se, Te, F, and, partially, N. The highest content of nitrogen in a spinel reported until now is rather low, however, and found for γ-aluminum oxynitride (AlON), a solid solution phase which can incorporate up to 15% N atoms on the X atom sites at 2123 K (4, 5). Numerous spinels contain first-row transition metals on the A and/or B sites, and these have been extensively studied with respect to magnetic properties (6), both for material applications and as model systems for magnetic interactions (7). New combinations of mixed valancies and uncommon stoichiometries in spinels can be achieved given the feasibility of a substitution of N^{3-} for O^{2-}. Such new spinels may well exhibit magnetic properties of interest. The present article treats the synthesis, structure, and magnetic properties of an oxynitride spinel $Mn_2(MnTa_3)N_{6-\delta}O_{2+\delta}$ ($0 \leq \delta \leq 1$) with a high nitrogen content.

EXPERIMENTAL

The Ta gels were prepared by dissolving $TaCl_5$ (Merck p.a.) in dry methanol and hydrolyzing the solutions by rapid injection of water. Hydrolysis was carried out both under acidic and basic conditions, the latter achieved by adding NH_3 to the water. Xerogels were obtained by evaporation of the solvent on a hot plate. The Ta content of the gels was determined thermogravimetrically by recording the weight loss upon heating in air to 1275 K, the end product being Ta_2O_5. A more detailed description of the preparation and characterization of the gels as well as the reaction chamber for the ammonolysis is given in Ref. (1).

Samples for the phase analysis studies were prepared by heat treating ground mixtures of Ta gel, hydrolyzed under acidic conditions, and Mn(II)–acetate, in an ammonia atmosphere at 973, 1073, and 1173 K. The Mn content in the mixtures, relative to Mn + Ta, was 10, 33.3, 50, and 66.7 at% Mn. The mixtures were placed in Pt, Au, or Al_2O_3 cups, each containing 20–50 mg. The samples were heated to 973 K for 2–3 hr, held at 973 K for 1 day, and then heated to and held at the final temperatures for 3 days. The heat treatment was ended by allowing the samples to cool to room temperature in the furnace, over a period of 12 hr.

[1] To whom correspondence should be sent.

0022-4596/95 $6.00

The formation of the spinel phase was not observed to be dependent on the hydrolyzing conditions of the Ta gels. Only gels hydrolyzed under basic conditions were used in subsequent preparations of the spinel, however.

Approximately 25 g of the spinel phase was needed for the neutron diffraction studies. The amount was prepared in successive 5-g batches in an Al_2O_3 boat at 1173 K. For these larger scale preparations it was necessary to increase the final heat treatment by 2 to 3 days, with intermediate regrindings, in order to obtain homogeneous samples.

A JEOL JSM 820 scanning microscope and a JEOL JEM-2000 FX-II transmission electron microscope, equipped with EDX (energy-dispersive X ray) microanalysis systems, LINK AN 10000 and LINK QX200 respectively, were used in characterizations of the ammonolyzed materials.

XRPD (X ray powder diffraction) patterns were recorded with a focusing camera of Guinier-Hägg type, using Cu$K\alpha_1$ radiation and Si as internal standard. The films were evaluated with a film scanner system (8). XRPD data for Rietveld refinements were collected with a STOE STADI/P diffractometer, using Cu$K\alpha_1$ radiation and a linear position-sensitive detector covering 4.6° in 2θ.

Neutron powder diffraction data were collected, both at room temperature and 15 K, at the Swedish research reactor R2 in Studsvik. A double monochromator system (Cu(220)) was set to give a wavelength of 1.470 Å. After collimation ($\alpha_1 = 10'$ and $\alpha_2 = 12'$), the neutron flux at the sample position was $\approx 10^6$ cm^{-2}sec^{-1}. The sample had a size of about 3 cm^3 and was contained in a vanadium tube ($\phi = 9$ mm). The instrument had an array of 10 detectors spaced 3.12° apart. All detectors scanned over each point in 2θ, and the intensities were added. Statistical analysis of the different contributions to each observed step intensity showed no anomalies. Data were collected between 10° and 128°.

Thermal analysis was performed with a Setaram TAG 24 analyzer, operated in air with a heating rate of 10°C min^{-1}.

Magnetic measurements were carried out in a weak field ac-susceptometer (Lake Shore 7130) in the temperature range 15–260 K, using magnetic fields between 250 and 500 A · m^{-1} and frequencies between 125 and 500 Hz.

RESULTS

Phase Analysis

The XRPD patterns of samples heat treated at 1073 and 1173 K contained reflections which could be indexed with a cubic face-centered cell with $a \approx 8.84$ Å. Samples with 50% Mn exhibited no additional reflections if Al_2O_3 cups were used as sample containers, but a few reflections from Ta_3N_5 appeared when Au or Pt cups were used. The cell dimensions obtained are $a = 8.8353(3)$ Å, $V = 689.7$ Å^3. The indexed powder pattern is given in Table 1. The reflection intensities were found to agree with a spinel structure having a cation distribution $Mn(Mn_{1/2}Ta_{3/2})(O,N)_4$. The color of the spinel ranged from brown to dark brown. Darker samples were obtained for longer heat treatments and/or higher temperatures. A preparation with 47% Mn yielded an X ray monophasic sample, indicating that the spinel extends toward Ta-rich compositions. The cell dimensions did not show any significant variation with composition, however.

TABLE 1
Powder X Ray Diffraction Pattern of $Mn_2(MnTa_3)N_{6-\delta}O_{2+\delta}$, $0 \le \delta \le 1$

hkl	$2\theta_{obs}$	$\Delta 2\theta$	d_{obs} (Å)	I/I_0 (%)
1 1 1	17.379	0.008	5.10	44
2 2 0	28.562	0.010	3.123	7
3 1 1	33.616	0.000	2.664	100
2 2 2	35.159	0.002	2.550	46
4 0 0	40.826	0.005	2.2085	36
3 3 1	44.668	−0.003	2.0271	14
4 2 2	50.548	−0.022	1.8042	2
5 1 1/3 3 3	53.875	0.000	1.7004	38
4 4 0	59.104	0.003	1.5618	47
5 3 1	62.104	0.003	1.4934	12
6 2 2	69.741	0.002	1.3473	15
4 4 4	70.663	−0.001	1.3320	25
7 1 1/5 5 1	74.322	0.003	1.2752	9
6 4 2	77.005	−0.011	1.2373	7
7 3 1/5 5 3	81.472	0.022	1.1804	1
8 0 0	84.075	−0.009	1.1504	25
	88.447	−0.003	1.1044	9

Note. $\Delta 2\theta = 2\theta_{obs} - 2\theta_{calc}$. $\lambda = 1.5406$ Å. $a = 8.8353(3)$ Å, $V = 689.7$ Å^3. Cell figure-of-merit $M_{17} = 250$, $F_{17} = 123$ (0.00630, 22). Reflection intensities originate from diffractometer data.

The powder patterns of samples with 10 and 33.3% Mn contained reflections from Ta_3N_5 in addition to the spinel reflections and, when prepared at 1173 K, one or two additional unidentified weak reflections. Samples with 66.7% Mn contained the spinel phase and a cubic face-centered phase with an a axis very close to half of that of the spinel. Its presence was first noted as a broadening and shift in the intensity distribution of the spinel reflections. The phase was subsequently obtained fairly pure at 1175 K in samples containing 80% Mn. The reflection intensities accord with an NaCl-type phase. The observed cell dimensions, $a = 4.4382(3)$ Å, $V = 87.42$ Å^3, are similar to, but smaller than those for MnO ($a = 4.445$ Å, JCPDS 7-230). Electron diffraction patterns showed, however, superstructure reflections corresponding to a doubling of the unit cell. The larger scale quantity of the spinel phase used for the neutron diffraction work contained a small amount of the NaCl-type phase as an impurity (cf. below).

Preparations at 973 K yielded only small amounts of the spinel phase. The sample with 66.7% Mn was black and yielded a powder pattern which could be indexed with a hexagonal cell with $a = 5.3024(4)$, $c = 14.493(2)$ Å, $V = 352.9$ Å^3. The cell is similar to that reported for the pale pink oxide $Mn_4Ta_2O_9$ (9, 10) ($a = 5.337$, $c = 14.333$ Å), but reflection intensities are different. The XRPD data indicate on ilmenite ($FeTiO_3$)-type structure with a cation distribution according with the formula $Mn(Mn_{1/3}Ta_{2/3})(O,N)_3$. Further studies of this phase are presently in progress.

Compositional and Thermogravimetrical Analysis

SEM investigations showed that the monophasic spinel phase samples consisted of fine grains, typically less than 100 nm in size. EDX analysis yielded a metal composition of 49(2)% Mn and 51(2)% Ta. The good agreement with the nominal composition, and the absence of any signal from Cl, indicates that all Cl escaped as NH_4Cl during the ammonolysis.

The TG and DTA curves showing the oxidation of the spinel phase in air are given in Fig. 1. The XRPD pattern of the end product at 1300 K showed it to consist of $MnTa_2O_6$ and Mn_3O_4. A weight increase occurs up to ca. 740 K, associated with an oxidation and simultaneous loss of N. The DTA curve shows that the exothermic oxidation reaction takes place in two steps. The sample weight decreases in the temperature interval from 740 to 1300 K, via a plateau at ca. 1000 K. The δ value in $Mn_2(MnTa_3)N_{6-\delta}O_{2+\delta}$ was calculated from the observed weight change and was based upon the decomposition reaction; $2Mn_2(MnTa_3)N_{6-\delta}O_{2+\delta} + (9 - \delta)O_2 \Rightarrow 3MnTa_2O_6 + Mn_3O_4 + (6 - \delta)N_2$. Two TG recordings for samples of the same nominal composition, but originating from different preparations, yielded approximately the same δ value, 0.7 with an estimated accuracy of 0.3.

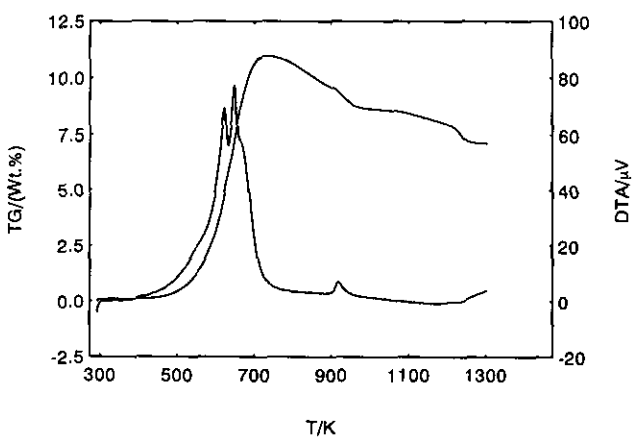

FIG. 1. TG and DTA curves for the oxidation of $Mn_2(MnTa_3)N_{6-\delta}O_{2+\delta}$, $0 \le \delta \le 1$, in air.

TABLE 2
Results from Combustion Analysis of the N and O Content in the Mn–Ta–(O,N) Spinel

Sample	% Mn	wt% N	wt% O	N_xO_y[a]
I	50	10.0(2)	4.2(2)	$N_{5.9}O_{2.2}$
II[b]	50	9.8(2)	5.3(2)	$N_{5.8}O_{2.8}$
III[c]	47	10.4(2)	4.1(2)	$N_{6.4}O_{2.2}$

[a] Calculated for a composition $Mn_2(MnTa)_4N_xO_y$. The esd in the obtained x and y is 0.2.
[b] From preparation used for neutron diffraction studies.
[c] Corresponding nominal composition $Mn_2(Mn_{0.82}Ta_{3.18})N_xO_y$.

Three samples were sent to a commercial laboratory (Sandvik AB) for combustion analysis of N and O content. The results are given in Table 2. Sample II was taken from the quantity used for powder neutron studies and sample III from an X ray monophasic preparation with 47% Mn and corresponding nominal composition $Mn_2(Mn_{0.82}Ta_{3.18})(N,O)_8$. The analyses yield total anion contents which are somewhat higher than allowed by an $(A,B)_3X_4$ stoichiometry. In this connection it can be noted that a similar discrepancy was observed for analysis of samples in the Ta–Zr–(O,N) system (1). The results may be interpreted in two ways. If they are regarded as correct, they indicate a cation deficiency in the spinel and a δ value between 0.2(2) and 0.6(2). If, on the other hand, one assumes that the N content is correct, but that the O content is due to systematic errors, e.g., a surface adsorption of H_2O, the analyses are more consistent and yield a δ value in $Mn_2(MnTa_3)N_{6-\delta}O_{2+\delta}$ of 0.1(2).

X Ray and Neutron Powder Diffraction

The spinel structure of $Mn_2(MnTa_3)N_{6-\delta}O_{2+\delta}$ was refined from XRPD data, using a local version of the DBW.2S Rietveld program (11). The final refinement was carried out with a total of 20 parameters. The number of theoretical Bragg reflections for $2\theta < 123°$ was 39, and the half-width of the peaks was 0.26° at $2\theta = 50°$. The atoms are distributed over the following sites in space group $Fd3m$ (origin at $3m$); 1 Mn at 8(a) at (1/8, 1/8, 1/8), 0.25 Mn and 0.75 Ta at 16(d) at (1/2, 1/2, 1/2), and 0.663 N and 0.337 O at 32(e) at (x, x, x), $x \approx 1/4$. The corresponding R values obtained were $R_p = 2.2$, $R_{wp} = 3.0$, $R_I = 2.8$, and $R_F = 1.9\%$. Alternative cation distributions yielded a poorer fit between observed and calculated intensities. The positional x parameter for the anions refined to 0.25(2), i.e., to a value indiscernible from the ideal value of 1/4 for a perfect cubic close packing of the anions. The refinement validates the structural model with respect to the distribution of cations, whereas the anion positions are not accurately determined, due to the dominating X ray scattering power of the metal atoms.

TABLE 3
Structural Parameters Refined from Neutron Powder Diffraction Data at 295 K for $Mn_2(MnTa_3)N_{6-\delta}O_{2+\delta}$, $0 \le \delta \le 1$

Atom	Site	x	y	z	β (Å^2)	Occupancy
Mn	8(a)	1/8	1/8	1/8	1.7(2)	1.0
Mn	16(d)	1/2	1/2	1/2	1.5(1)	0.25
Ta						0.75
N	32(e)	0.2618(2)	0.2618	0.2618	1.8(1)	0.65(6)
O						0.35(6)

Powder neutron diffraction data were collected, both at room temperature and 15 K, in order to achieve a better determination of the anion positions and also to reveal a possible magnetic ordering of the Mn atoms.

The structure was refined from room temperature neutron powder diffraction data and 47 theoretical reflections in the 2θ range 10° to 128°. The sample contained a smaller amount of the NaCl-type Mn–Ta (oxy)nitride phase, which was included as a second phase in the refinement with a hypothetical composition of $(Mn_{0.8}Ta_{0.2})N$. A total of 23 parameters were included in the final refinement. For the spinel phase 11 parameters were refined: a scale factor, the unit cell dimension, 3 (U, V, W) half-width parameters, 1 peak asymmetry parameter, 3 temperature factors, the anion positional parameter, and the relative fraction of N and O atoms, assuming full occupancy of the sites. For the impurity phase 4 parameters were used: the scale factor, the cell dimension, 1 overall temperature factor, and 1 uncoupled W parameter. The remaining 8 parameters were the zero-point, 6 background polynomial coefficients, and the η mixing coefficient for the chosen pseudo-Voigt profile function.

The refined structural parameters are given in Table 3, with the esd obtained in the refinement multiplied by 1.75 in order to account for serial correlation (12) (Durbin–Watson D value = 1.24). The refined site occupancy factor (sof) for N, 0.65(6), corresponds to a δ value in $Mn_2(MnTa_3)N_{6-\delta}O_{2+\delta}$ of 0.8(5). Corresponding selected bond distances are given in Table 4. The agreement between calculated and observed diffraction patterns is shown in Fig. 2. The corresponding R values are R_p = 4.4, R_{wp} = 5.5, R_I = 2.9, and R_F = 2.7%, and the goodness-of-fit value is S = 1.30. The peak half-width is 0.30° in 2θ

TABLE 4
Atomic Distances (Å) in $Mn_2(MnTa_3)N_{6-\delta}O_{2+\delta}$, $0 \le \delta \le 1$, at 295 K

Mn–(O,N)	×4	2.093(2)	(O,N)–(O,N)	×3	2.829(3)
				×6	3.131(2)
(Mn,Ta)–(O,N)	×6	2.110(2)		×3	3.419(3)
				Average	3.128

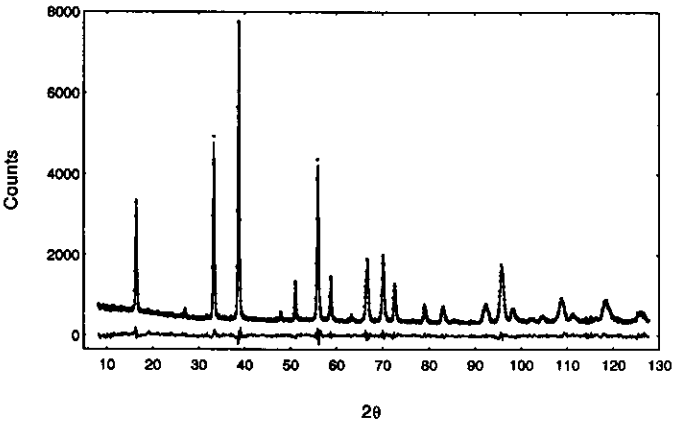

FIG. 2. Observed (points), calculated (solid line), and difference (bottom) neutron diffraction pattern of $Mn_2(MnTa_3)N_{6-\delta}O_{2+\delta}$, $0 \le \delta \le 1$, at 295 K.

at 2θ = 33.5° and 1.77° at 2θ = 127°. The pseudo-Voigt mixing parameter η refined to 0.40(5). The peaks thus contain an appreciable Lorentzian contribution, as seen in the part of the pattern shown in Fig. 3. They are furthermore slightly asymmetric toward high 2θ, yielding a refined asymmetry parameter of −0.12(2). The impurity phase refined to R_F = 2.0%, with β = 1.5(4) Å^2 and a scale factor of 0.020(2), compared with 0.234(2) for the spinel. The scale factors indicate an amount of impurity phase of ca. 0.1 wt%, using the formula $w_j = S_j Z_j M_j V_j / \sum S_j Z_j M_j V_j$, w_j being the weight fraction, S_j the scale factor, Z_j the number of formula units per cell, M_j the mass of the formula unit, and V_j the unit cell volume for phase j.

A number of additional refinements were made, which all yielded similar or slightly higher R values. A refinement

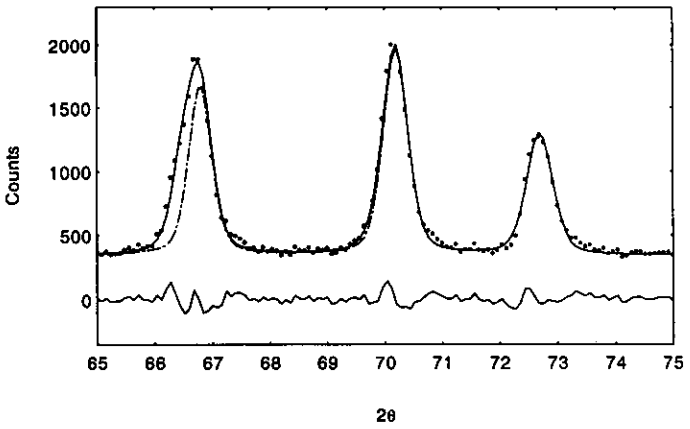

FIG. 3. Expanded portion of the neutron powder pattern of $Mn_2(MnTa_3)N_{6-\delta}O_{2+\delta}$, $0 \le \delta \le 1$, at 295 K. Data points are shown by small circles. The solid line represents the calculated pattern, including the impurity phase, and the dotted line a corresponding pattern without the impurity phase. The spinel 226 reflection at 2θ = 66.9° ($I/I_0 \approx 27\%$) is overlapped by the impurity 113 reflection at 2θ = 66.6° ($I/I_0 \approx 82\%$).

of the ratio of Mn and Ta on the octahedral sites validated the presumed cation distribution and yielded an sof of 0.73(2) for Ta. The data were furthermore inspected for indications of cation vacancies. There cannot be vacancies solely at the tetrahedral sites, if these sites are occupied only by Mn atoms, without changing the Mn : Ta ratio of the octahedral sites from the ratio 1 : 3. A refinement allowing for vacancies at octahedral sites only, while retaining an overall cation stoichiometry, yielded only very minor changes in residual R factors and a total sof on octahedral sites of 0.92(4). A refinement allowing for vacancies at both octahedral and tetrahedral sites gave larger R values and sof's above one. The use of anisotropic temperature factors was tested, but yielded no improvements.

The neutron powder pattern recorded at 15 K was similar to the room temperature pattern. There was no distinct change of peak intensities, nor any appearance of additional super-cell reflections, caused by a magnetic order, notwithstanding the fact that the data were collected at a temperature well below the observed magnetic transition temperature of 29 K (see below). A refinement corresponding to the room temperature one yielded somewhat higher structure R factors, $R_I = 4.1$ and $R_F = 3.6\%$, and slightly lower profile R factors, $R_p = 4.1$ and $R_{wp} = 5.2\%$. The smaller values of the latter are, at least partly, attributable to a higher background of incoherent scattering. The refined anion x parameter remained unaltered, while a lower value value of the nitrogen content was obtained, sof for N = 0.47(8). The refined cell parameter at 15 K was 8.8311(8) Å, compared with 8.8446(6) Å obtained at room temperature. The discrepancy between observed and calculated intensities were, for the 15 K data, slightly larger for low-angle reflections. Exclusion of the first two reflections thus resulted in a lower R_I value by 0.4% units, while such an effect was not observed for the room temperature data. Since the 15 K data were recorded below the magnetic transition temperature, it is conceivable that they contain an intensity contribution from a magnetic order, in which case the lower angle reflections would be affected most. We therefore conclude that the room temperature refinement gives the more reliable structure determination and that the intensity contribution of a long-range magnetic order, if any, is too small to be used to determine such an order.

Magnetic Susceptibility

Alternating current susceptibility curves, obtained in the temperature interval 15–260 K (125 Hz, 250 $A \cdot m^{-1}$) are shown in Figs. 4a (χ_M vs T) and 4b (χ_M^{-1} vs T), with χ_M denoting the molar susceptibility. Susceptibility data collected at different frequencies and fields yielded identical curves. Two important features can be noted in these

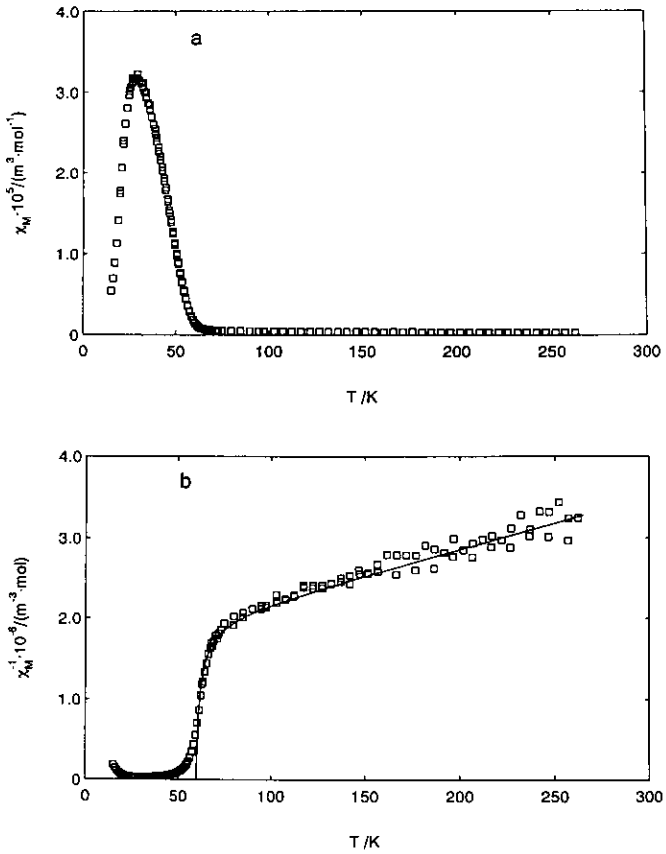

FIG. 4. The molar magnetic susceptibility (a), and inverse molar magnetic susceptibility (b), versus temperature for $Mn_2(MnTa_3)N_{6-\delta}O_{2+\delta}$, $0 \leq \delta \leq 1$. The solid line in (b) shows the fit of the data to Eq. [1].

curves. At 29 K a well-defined peak can be observed (Fig. 4a), and above that temperature the behavior appears paramagnetic (Fig. 4b).

Many spinels containing magnetic ions are ferrimagnetic or antiferromagnetic (e.g., ferrites), and a test was made to see whether the Néel equation for a two—sublattice ferrimagnet could be fitted to the susceptibility curve, i.e.,

$$\frac{1}{\chi_M} = \frac{1}{C}\left[T - \theta_a - \frac{\theta_b^2}{T - \theta}\right]. \qquad [1]$$

In this equation $C = C_1 + C_2$, C_1 and C_2 being the Curie constants for the tetrahedral and octahedral sublattices, respectively; T is the absolute temperature; and θ_a, θ_b, and θ are various constants, as defined in Ref. (7). Fitting Eq. [1] to the paramagnetic part of the curve yielded the following values of the constants: $C = 1.56(7) \times 10^{-4}$ $m^3 \cdot K \cdot mol^{-1}$, $\theta_a = -250(20)$ K, $\theta_b^2 = 610(90)$ K, and $\theta = 57.6(2)$ K. However, as no low temperature magnetic or-

der was revealed by the neutron data (at 15 K) the above ferrimagnetic interpretation is somewhat dubious, and the true nature of the observed magnetic transition at 29 K remains unclear.

From the Curie constant the effective number of Bohr magnetons per Mn ion (μ_{eff}) was determined to be 5.7(2). The expected values for Mn^{2+} and Mn^{3+}, in a high-spin (hs) state, are 5.9 and ca. 4.9 μ_B, respectively. It may be remarked that the μ_{eff} value obtained was quite sensitive to the applied correction for signal contributions not originating from the sample, e.g., from the sample holder.

Electrical Conductivity

The electrical conductivity of a pressed rod of $Mn_2(MnTa_3)N_{6-\delta}O_{2+\delta}$ was measured between 160 and 295 K, by the four-probe method. A semiconductor behavior was observed, with an activation energy of 0.14 eV and a conductivity of ca. $2 \cdot 10^{-7}\ \Omega^{-1}cm^{-1}$ at room temperature.

DISCUSSION AND CONCLUSIONS

The $Mn_2(MnTa_3)N_{6-\delta}O_{2+\delta}$ phase is the first reported oxynitride spinel in addition to γ-aluminum oxynitride (AlON). The portion of N anions is, however, considerably higher in the Mn–Ta spinel (63–75%) than in AlON (up to ca. 15%). A recent article by Elder *et al.* (13) discusses the thermodynamic aspects of nitride formation from corresponding oxides. The authors conclude that if binary (oxy)nitrides are stable relative to their oxides, then the ternary (oxy)nitrides are, probably, stable as well. The stability of the $Mn_2(MnTa_3)N_{6-\delta}O_{2+\delta}$ phase may accordingly be understood in view of the number of known (oxy)nitrides containing Mn and Ta (14), where several of the latter ones are compounds with Ta^{5+} ions. The results of the phase analysis indicate that the spinel phase extends toward Ta-rich compositions. We have, however, not been able to prepare a phase of the composition $MnTa_2N_4$ by using the present synthesis method.

According to the TG data, the Rietveld refinement data, the combustion analysis, and the magnetic susceptibility measurements, the composition of the spinel is found to be between $Mn_2(MnTa_3)N_6O_2$ ($\delta = 0$) and $Mn_2(MnTa_3)N_5O_3$ ($\delta = 1$). Full occupancy of the cation sites is hereby assumed (cf. below). These limits correspond, per formula unit, to 2 Mn^{2+} and 1 Mn^{3+} for $\delta = 0$, and to 3 Mn^{2+} for $\delta = 1$. The thermogravimetric analysis yielded $\delta = 0.7(3)$ and the room temperature neutron data $\delta = 0.8(5)$. The combustion analysis of the O and N content gave a δ value between 0.1(2) and 0.6(2), depending on how the analysis results were interpreted. The magnetic susceptibility measurements yielded a magnetic moment of 5.7(2) μ_B per Mn above the transition temperature of 29 K. The values expected from the composition, assuming hs Mn ions, are 5.9 μ_B for only Mn^{2+} ($\delta = 1$) and ca. 5.6 μ_B for Mn^{2+} on the *A* sites and Mn^{3+} on the *B* sites ($\delta = 0$). The measured μ_{eff} agrees, within experimental error, with both these possibilities. The spinel may, furthermore, well exhibit a variable δ value, as indicated also by the different colors of the preparations.

The XRPD and neutron powder diffraction data show unequivocally that the tetrahedral *A* sites are occupied only by Mn atoms and that the octahedral *B* sites are occupied by ≈ 1/4 Mn and ≈3/4 Ta atoms. Since Mn^{3+} has a high preference for the octahedral sites in spinels (7), it is reasonable to assume that the *A* sites are occupied by only Mn^{2+}, in a hs state, and that any Mn^{3+} present is located on the *B* sites. A partial occupancy of the *B* sites by Mn^{3+} is not expected to cause any cooperative Jahn-Teller distortion of the cubic structure (7).

As in most spinels the *A* and *B* sites in $Mn_2(MnTa_3)N_{6-\delta}O_{2+\delta}$ are of similar size. The corresponding cation–anion distances are 2.093(2) and 2.110(2) Å, respectively. If an average anion radius of 1.43 Å is used, then these distances correspond to average cation radii of $r_A = 0.66$ Å and $r_B = 0.68$ Å. The former agrees well with a radius of 0.66 Å for four-coordinated hs Mn^{2+} (15). The *B* sites are slightly larger than would be expected from the radius of Ta^{5+} alone, 0.64 Å. The r_B value 0.68 Å accords reasonably well with a weighted average of the radii of six-coordinated hs Mn^{2+} (0.83 Å) and Ta^{5+} (0.64 Å), 0.69 Å, and indicates thus a δ value close to 1.

The neutron powder patter collected at 15 K exhibited no apparent evidence of a magnetic ordering of the Mn ions. One possible explanation for this is that the magnetic interactions are of a short-range character. The observed large ratio between θ_a and the transition temperature, $-250/29 = -8.6$, is indicative of magnetic frustration (16). Another, less likely, possibility seems to be that the spins are ordered, but arranged in a manner that does not produce any substantial magnetic contribution to the reflection intensities, as is apparently the case for the spinel $AlVO_3$ (17).

The 1 : 1 cation ratio in $Mn_2(MnTa_3)N_{6-\delta}O_{2+\delta}$ is rare for spinels. Several compounds having the spinel structure and an ABX_3 stoichiometry have, however, been reported (3): $AlVO_3$, $CoTiO_3$, $ZnTiO_3$, $CdSnO_3$, and $ZnMnO_3$. These spinels have cation vacancies at the *A* and/or *B* sites. The neutron powder data for $Mn_2(MnTa_3)N_{6-\delta}O_{2+\delta}$ indicate that a smaller concentration of vacancies, ca. 8(4)%, may exist at the octahedral *B* sites. The combustion analysis of the O and N content yielded, moreover, for two of the three samples analyzed, a total anion content exceeding that for an $(A,B)_3X_4$ spinel stoichiometry. These analysis results may be interpreted as indications of cation vacancies. However, if δ in $Mn_2(MnTa_3)N_{6-\delta}O_{2+\delta}$ is between 0 and 1 and the *A* sites contain only Mn^{2+}, then

the maximum possible vacancy concentration at the *B* sites is 6.25%, corresponding to the formula $Mn_2^{2+}(Mn_{0.875}^{3+}Ta_{2.875}^{5+}\square_{0.22})N_5O_3$. This amount is substantially less than for a spinel with an ABX_3 stoichiometry, 16.7%.

ACKNOWLEDGMENTS

The authors thank Mr. A. Sjödin for help with the synthesis work, Dr. T. Hörlin for the electrical conductivity measurement, Dr. R. Tellgren (Studsvik) for providing the facilities for the neutron diffraction work, Mr. H. Rundlöf (Studsvik) for assistance with the collection of neutron diffraction data, and Professor M. Nygren for support and valuable discussions.

REFERENCES

1. J. Grins, P.-O. Käll, and G. Svensson, *J. Mater. Chem.* **4**(8), 1293 (1194).
2. N. N. Greenwood, "Ionic Crystals, Lattice Defects and Nonstoichiometry," Chap. 5. Butterworth, London, 1968.
3. O. Muller and R. Roy, "The Major Ternary Structural Families," Chaps. 2 and 4. Springer-Verlag, Berlin/New York, 1974.
4. H. X. Willems, M. M. R. M. Hendrix, G. deWith, and R. Metselaar, *J. Eur. Ceram. Soc.* **10,** 346 (1992).
5. H. X. Willems, G. deWith, R. Metselaar, R. B. Helmholdt, and K. K. Petersen, *J. Mater. Sci. Lett.* **12,** 1470 (1993).
6. K.-H. Hellwege and A. H. Hellwege, Eds., "Landolt-Börnstein, Series III," Vols. 4(b) and 12(b). Springer-Verlag, Berlin/Heidelberg, 1970 and 1980.
7. J. B. Goodenough, "Magnetism and the Chemical Bond." Wiley, New York/London, 1963.
8. K. E. Johansson, T. Palm, and P.-E. Werner, *J. Phys. E* **13,** 1289 (1980).
9. A. C. Turncock, *J. Amer. Ceram. Soc.* **49**(7), 382 (1966).
10. E. F. Bertaut, L. Corliss, F. Forrat, R. Aleonard, and R. Pauthenet, *J. Phys. Chem. Solids* **21**(3), 234 (1961).
11. D. B. Wiles, A. Sakthivel, and R. A. Young, "Users Guide to Program DBW3.2S for Rietveld Analysis of X-ray and Neutron Powder Diffraction Data Patterns (Version 8804)." School of Physics, Georgia Institute of Technology, Atlanta.
12. J.-F. Berar and P. Lelann, *J. Appl. Crystallogr.* **24,** 1 (1991).
13. S. H. Elder, F. J. DiSalvo, L. Topor, and A. Navrotsky, *Chem. Mater.* **5,** 1545 (1993).
14. N. E. Brese and M. O'Keeffe, *Struct. Bonding* **79,** 309 (1992).
15. R. D. Shannon, *Acta Crystallogr. Sect. A* **32,** 751 (1976).
16. A. P. Ramirez, *Annu. Rev. Mater. Sci.* **24,** 453 (1994).
17. A. F. Reid and T. M. Sabine, *J. Solid State Chem.* **2,** 203 (1970).